Hydroxylation of Actin Impairs Cell Motility Through Blocking its' Histidine Methylation

Zhenzhen Zi [1], Lin Yuan [1], Qing Ding [1,2], Chiho Kim[1], Xu-dong Wang[1], Xiaoyu Zhang [1], and Yonghao Yu [1, *]

1. Department of Biochemistry, UT Southwestern Medical Center, Dallas, Texas, USA.

2. Children's Research Institute and the Department of Pediatrics, University of Texas Southwestern Medical Center, Dallas, Texas, USA

* Correspondence should be addressed to Y.Y.

E-mail: Yonghao.Yu@UTsouthwestern.edu,

Telephone: 214-648-3535

Keywords:

MK-8617, Cell Motility, Actin, Histidine Methylation, Proline Hydroxyproline,

Mass Spectrometry

Abstract:

Protein hydroxylation is a post translational modification happens on various amino acids, which is catalyzed by the oxoglutarate and oxygen dependent dioxygenases. The best characterized hydroxylated protein is the hypoxia inducible factor (HIF), which is degraded by VHL/elongin C/elongin B/cullin 2/RBX1 (VCB/CR) E3 complex under normal oxygen conditions. Hypoxia or inhibitors (including FG4592 and MK8617) of PHDs stabilize HIF1a and regulate its downstream targets. Prolyl hydroxylase, including PHD2 and PHD3 has been reported in regulating actin polymerization and cell motility. Here, we found MK8617 regulated cell motility in Von Hippel Lindau (VHL) dependent manner. Through the protein hydroxylation proteome experiment upon MK8617 treatment, we identified Pro70 in actin could be hydroxylated and near to His73, which has been reported be methylated and stabilize actin polymerization. Using biochemical assay, we found that binding of VHL with hydroxylated actin (Pro70) decrease the His73 methylation by blocking the interaction of actin with SETD3, the His73 methyltransferase, and further regulated actin polymerization and cell motility. In summary, our study revealed that

hypoxia and deficiencies in the VHL, in a HIF independent and prolyl hydroxylation dependent manner, regulate actin polymerization and cell motility through the PTM (Post Translational Modifications) crosstalk.

Introduction:

Protein hydroxylation is a post-translational modification occurs on various amino acids, including proline, lysine, asparagine, aspartate and histidine (1). The proline hydroxylation reaction is catalyzed by the 2-oxoglutarate- and oxygen-dependent dioxygenases PHD1, PHD2, and PHD3 (2). A well-known example of hydroxylation is hypoxia inducible factor alpha (HIF-1α, at Pro 402 and 564), which regulate HIF-1α stability via the VHL-elongin C-elongin B-cullin 2-RBX1 (VCB-CR) E3 complex (3). Hypoxia-inducible factor (HIF) is a transcription factor involved in erythropoiesis, angiogenesis, glycolytic energy metabolism, and apoptosis (4). Besides HIF-dependent functions, VHL also play roles in the regulation of the extracellular matrix; microtubule stabilization and maintenance of the primary cilium; regulation of apoptosis; control of cell senescence; and transcriptional regulation (5).

Hypoxia or inhibitors (including FG-4592 and MK-8617) of PHDs stabilize HIF and regulate its' downstream targets (6). Small-molecule PHD enzyme inhibitors can efficiently activate HIF in the presence of oxygen (7-9). These small molecules could be therapeutically useful for a range of indications, most obviously for the treatment of anemia that results from impaired erythropoietin production (7). Activation of HIF is beneficial in ischaemic or ischaemia–reperfusion settings, as HIF acts upstream of diverse gene products that should be protective in these contexts by promoting vasodilatation and angiogenesis, increasing glucose uptake, modulating mitochondrial metabolism and decreasing free radical production (10). PHD enzyme inhibitors might also be of benefit in wound healing, stroke, myocardial ischaemia, limb ischaemia, acute kidney injury, and cell motility (7).

Actin is a conserved cytoskeletal protein that forms filaments and plays an essential role in cell movement (11). Two forms of actin exist in cells, including monomeric (G-actin) and filamentous (F-actin), the polymerization of G-actin into F-actin provides intracellular mechanical support that facilitates cell migration (11,12). Actin undergoes various forms of posttranslational modifications, which regulate the balance between G-actin and F-actin (13), including phosphorylation of Tyr-53, ADP-ribosylation of Arg-177 and Arg-206,

glutathionylation, carbonylation, or nitrosylation of Cys-374, which inhibit actin polymerization, while transglutamination of Lys-50, methylation of His-73, ADP-ribosylation of Thr-148, and arginylation, which stabilize the F-actin (13). The His73 methylation of actin has been reported to be catalyzed by the methyltransferase, SET domain protein 3 (SETD3), and regulate smooth muscle contractility (14,15).

Here, we found that MK-8617, a PHD enzyme inhibitor, could regulate cell motility and actin oligomerization in VHL dependent manner. Through the hydroxylation modification proteome quantification analysis, we identified several hydroxylated-proline sites in actin, one of which is Pro70. Pro70 is close to His73, a position could be methylated and regulates actin polymerization. Through the biochemical assay, we found that binding of hydroxylated Actin (Pro70) with VHL could block the interaction of Actin with SETD3, thereby blocking the His73 methylation by SETD3, which subsequentially regulate actin polymerization and cell motility. Therefore, our studies revealed that hypoxia and deficiencies in the VHL, in a HIF-independent and prolyl hydroxylation–dependent manner, regulate actin polymerization and cell motility.

Results and Discussion:

MK-8617 Regulate Cell Motility and Actin Oligomerization in VHL Dependent Manner

MK-8617, a pan-inhibitor for PHD enzymes, have been used to treat angiogenesis and other disease (6,16). As protein hydroxylation play a significant role in cancer cell invasion and metastasis, we examined whether MK-8617 influences cell motility. Through the cell scratch assay, we found that MK-8617 can promote cell motility only in Hela cells, but not in the 786-O or RCCJF cells (Fig. 1A). As 786-O and RCCJF cells are VHL null CCRCC cell lines, while Hela cells harbor normal VHL expression, this indicates that the effect of MK-8617 on cell motility is VHL dependent.

Actin exists in monomeric (G-actin) and filamentous (F-actin) forms in cells (12). Polymerization of G-actin into F-actin is critical for cell migration (11). Therefore, we measured the F-Actin level by using TRITC–conjugated phalloidin immunostaining. We found that MK-8617 promoted the F-actin formation in Hela cells, but not in VHL null 786-O cells (Fig. 1B). This is consistent with the cell motility response in Hela and 786-O cells upon MK-8617

treatment (Fig. 1A). His73 methylation in actin has been reported to stabilize actin polymerization (14). We found that the methylation level of actin-His73 was increased in Hela cells, while no change was observed in 786-O cells upon MK-8617 treatment (Fig. 1C and 1D). Same case applies to VHL positive HEK293T cells and VHL null RCCJF cells (Fig. 1E and 1F). These results indicate that MK-8617 regulates cell motility through regulating actin H73 methylation and actin polymerization, which is VHL dependent (Fig. 1G).

Protein Hydroxylation Proteome Response upon MK-8617 Treatment

MK-8617 is a common Hypoxia-inducible factor (HIF)-prolyl hydroxylase inhibitor (HIF-PHI) (6), we then investigated the whole proteome and hydroxylation proteome changes upon MK-8617 treatment in MCF10A cells, which has high PHDs expression level. We performed quantitative proteomic experiments (using the tandem mass tag, TMT6 labeling approach) in the MCF10A cells upon MK-8617 treatment at different time points (0/6/12/24/26/48 hours) (Fig. 2A). Under normal conditions, HIF1a is hydroxylated by the PHDs enzymes, and hydroxylated HIF1a is rapidly degraded by the von Hippel-Lindau–E3 ubiquitin ligase complex following ubiquitylation (2). Upon MK-8617 treatment, the degradation of HIF1a was inhibited, and this effect sustained for 48 hours (Fig. 2B, Table S1), which was consistent with the TMT-MS result (Fig. 2C). While the transcription of HIF1a has no response upon MK-8617 treatment (Fig. 2E), we found that BNIP3, a reported proapoptotic gene and a downstream target of HIF1a, could be induced upon MK-8617 treatment at transcriptional and protein levels (Fig. 2D and 2E, Table S1).

To characterize the whole hydroxylation-proteome perturbation upon MK-8617 treatment, we performed cluster analysis of the TMT-MS result. The results showed that the hydroxylation level of most proteins decreased upon 6 hours MK-8617 treatment and reached the lowest level upon 12 hours treatment (Fig. 2F). Of note, we observed that the hydroxylation motif was enriched in a poly-Proline sequence through the motif analysis based on the hydroxylated peptides identified using the TMT-MS analysis (Fig. 2G).

Among all the hydroxylated proteins, Actin (including alpha and beta actin) could be hydroxylated on several proline sites, including the Pro70 (Pro72 in ACTA)/102/109/164/258/264/307 (Fig. 3A, 3B and Table S2), of which Pro307 has been reported to be hydroxylated by PHD3 and play important roles in cell motility (17). To identify

which PHDs enzyme involve in actin hydroxylation, we performed co-immunoprecipitation assay, and found that actin can interact with PHD2 and PHD3, which indicates that actin could be hydroxylated by PHD2 and PHD3 (Fig. 3C). Notably, we found that Pro70, one of the hydroxylated proline sites in actin identified by the mass spectrometry responded well to PHD inhibition. The hydroxylation level of Pro70 significantly decreased upon 6- and 12-hours MK-8617 treatment (Fig. 3D), while the total actin protein amount has no change upon MK-8617 treatment (Fig. 3E).

The binding of VHL to Pro70-Hydroxylated Actin Inhibit His73 Methylation

We showed that MK-8617 treatment could downregulate Pro70 hydroxylation (Fig. 3D) while upregulate His73 methylation (Fig. 1C-1F), which indicates a correlation between actin Pro70 hydroxylation and His73 Methylation. As Histidine 73 in actin is methylated by SETD3, and we found that the interaction of actin and SETD3 could be enhanced by the Pro70 to Ala mutation (Fig. 3F). These results suggest a crosstalk between Pro70 hydroxylation and His73 methylation.

To investigate the role of Pro70 in His73 methylation, we then synthesized the hydroxylated peptide (Hyp70) and non-hydroxylated peptide (P70) (Fig. 3G). We found that only hydroxylated-Pro70 peptides bind to VHL but not the non-hydroxylated peptides (Fig. 3H). We further performed the in vitro methylation assay with these peptides. The results showed that P70 peptide had no changes on His73 Methylation levels with or without VHL incubation. However, the Hyp70 peptide showed significant lower levels of H73 methylation when incubated with VHL compared to that of VHL null condition (Fig. 3I). These results suggest that the hydroxylation on Pro70 of actin triggers the binding with VHL and therefore blocks the interaction of actin with SETD3, and subsequentially leads to the downregulated His73 methylation of actin.

VHL Regulates Cell Motility Through Regulating H73 Methylation

We found that knockdown of VHL in Hela cells with shRNA leads to an increase of actin polymerization and H73 methylation level compared to the control cells (Fig. 4A, 4B and 4C). In addition, knockdown of VHL also leads to an increase of cell motility (Fig. 4D). Meanwhile, the overexpression of VHL in VHL null 786-O cells leads to a decrease of actin polymerization compared to the control cells (Fig. 4A). Consistently, the cell motility will be blocked by the

overexpress of VHL in 786-O cells (Fig. 4E). These results indicated that, VHL could regulated F-Actin formation and cell motility through regulating the actin His73 methylation.

In summary, these results show a new mechanism about how VHL regulate cell motility (Fig. 4F). PHD2 or PHD3 hydroxylate Pro70 of actin, the hydroxylated actin binds to VHL and blocks the interaction between actin and SETD3, which subsequentially inhibits the His73 methylation. The downregulated H73 methylation then leads to the decreased F-actin formation and cell motility.

Discussion

The best-characterized function of VHL is that VHL mediates the degradation of the hydroxylated hypoxia-inducible factor (HIF) as a component of E3 ligase complex under normal oxygen conditions (3). The HIF independent functions of VHL are still poorly investigated. It's well recognized that the proline hydroxylation reaction is catalyzed by the 2-oxoglutarate- and oxygen-dependent dioxygenases PHD1, PHD2, and PHD3 (2). Inhibitors targeted to PHD enzymes have been used in anemia treatment, however, these inhibitors targeting to PHD proteins have pleiotropic effects, because these inhibitors will inhibit other 2-OG-dependent oxygenases (7). Here, we identified Actin as a direct hydroxylation substrate for PHD2 and PHD3 through the Co-immunoprecipitation assay (Fig. 3C) and found that the hydroxylation level of Actin Pro70 decreased upon MK-8617 treatment (Fig. 3B and 3D). Further analysis revealed that hydroxylated actin (Hyp70 peptide) binds to VHL (Fig. 3H).

Actin exists in both a monomeric globular state (G-actin) and a polymerized filamentous state (F-actin), and the switch between the two states is highly dynamic (12). The actin filaments play crucial roles in many cellular functions, including muscle contraction, cell signaling, as well as cell integrity and motility (18). Numerous studies and reviews describe the actin PTMs (post translational modifications) shedding light on a crucial aspect of actin biology (13). Extensive crosstalk between PTMs have been reported, which created a "PTM code" on proteins and could be recognized to regulate downstream events (19).

Actin hydroxylation site P70 is close to His 73, a critical site of actin, which could be methylated by SETD3, and regulate F-actin formation and cell motility. We observed that VHL binds to hydroxylated Pro70 actin and then blocks the binding of actin with SETD3, which

subsequentially prevents actin methylation on histidine 73, leading to a decrease of F-actin formation (Fig. 3). Indeed, the hydroxylation regulated cell motility is VHL-dependent, as MK-8617 treatment modulates His73 Methylation only in the VHL expressed cells (Hela or 293T cells), but not in the CCRCC cell lines (786-O and RCCJF), which have no VHL expression (Fig. 1). Here, we demonstrated that VHL knock down enhances cell motility in Hela cells and this phenomenon can also be validated by VHL overexpression in VHL null 786-O cells (Fig. 4). Thus, by identifying actin P70 as a hydroxylation target, we provide a mechanistic link between Pro70 hydroxylation and H73 methylation and reveal the role of VHL in this PMTs crosstalk. In summary, we unravel a novel molecular mechanism of F-actin formation and cell motility through VHL mediated inter-PMTs regulation.

Figures:

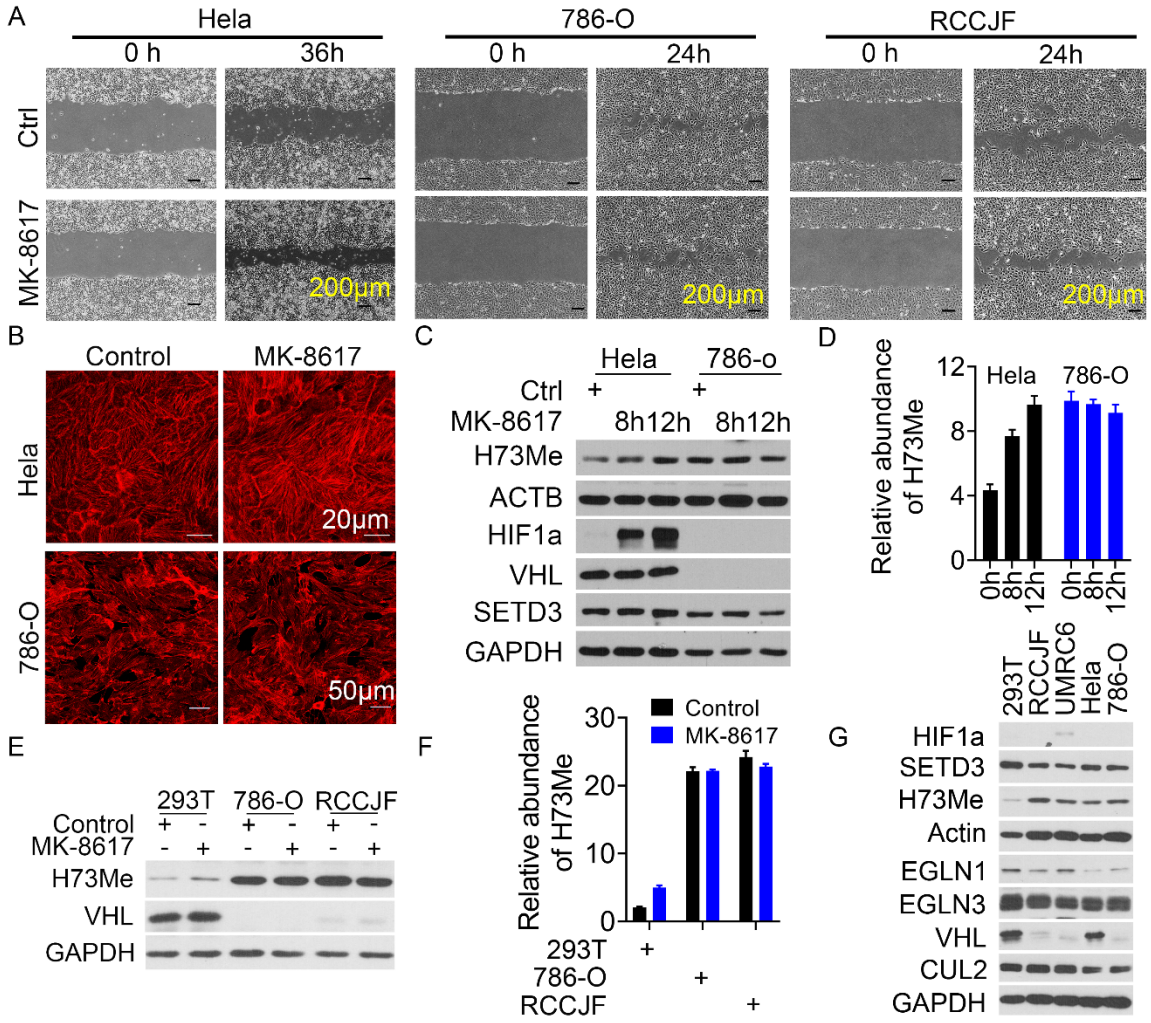

Fig. 1. MK-8617 Regulate Cell Motility and Actin H73 Methylation

A. MK-8617 promote cell motility in Hela cells but not in 786-O and RCCJF cells. Scratch assays were performed with Hela, 786-O and RCCJF cells under control and MK-8617 treatment (5μM). Representative images at indicated time points from two independent experiments. Scale bar, 200 μm.

B. MK-8617 increases β-actin polymerization in Hela cells but not in 786-O cells. HeLa and 786-O cells were treated with DMSO or MK-8617 (5 μM) for 24 h. Cells were fixed, permeabilized, stained with TRITC–conjugated phalloidin, and imaged by fluorescence microscopy. Scale bar, 50 μm.

(C-D). MK-8617 regulate H73Me-actin in Hela cells but not in 786-O cells. Hela and 786-O cells were treated with MK-8617 (5 μM) for indicated time points. Cell lysis were subjected to western blot (C) and H73Me level were quantified (D). GAPDH were used as the control.

(E-F). MK-8617 regulate H73Me-actin in Hela cells but not in 786-O and RCCJF cells. Hela, 786-O and RCCJF cells were treated with MK-8617 (5 μM) for 12 hours. Cell lysis were subjected to western blot (E) and H73Me level were quantified (F). GAPDH were used as the control.

G. Expression profile of HIF1a, SETD3, H73Me, Actin, EGLN1, EGLN3, VHL and CUL2 were measured in indicated cell lines. The same protein amount of indicated cells were subjected to western blot.

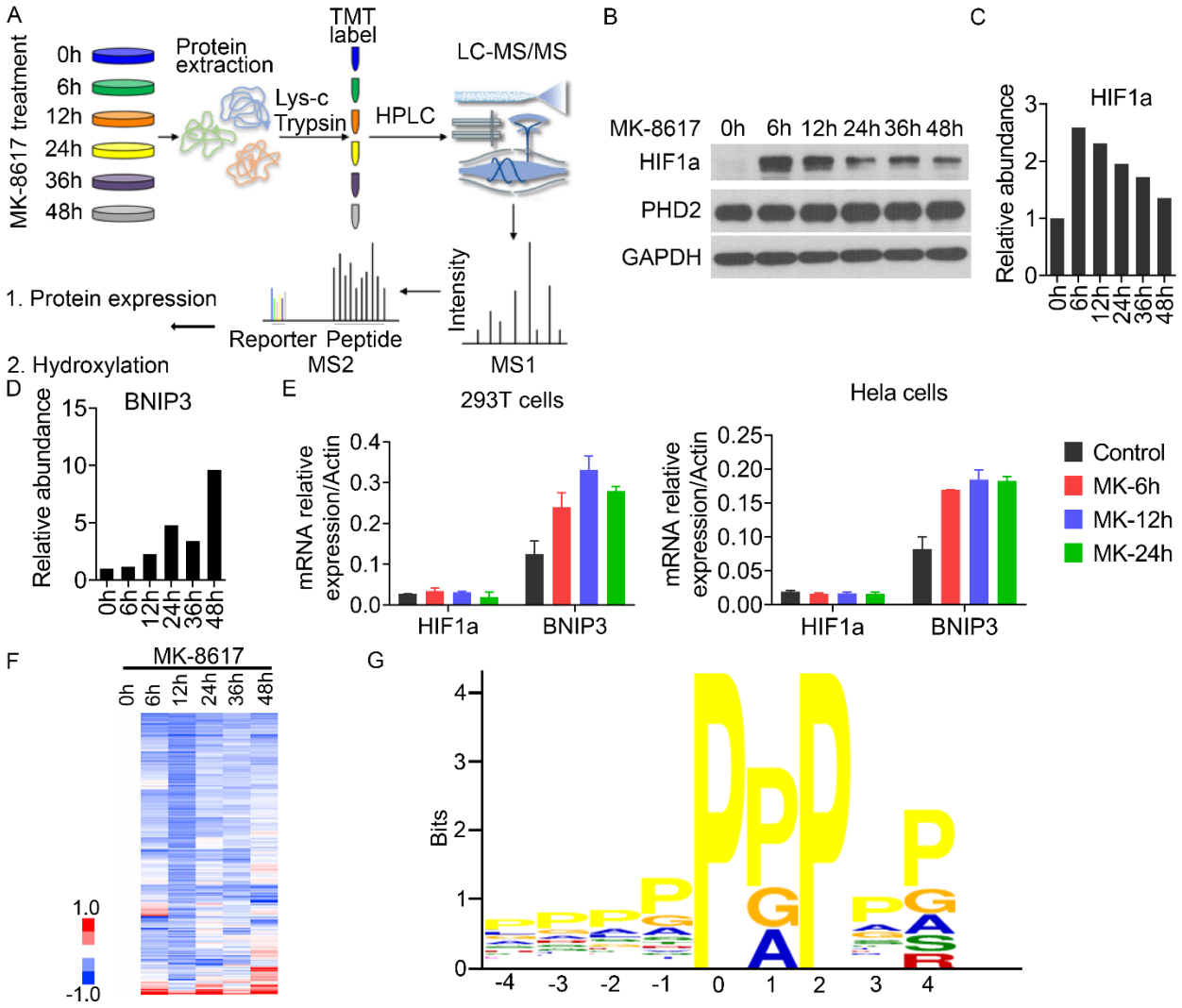

Fig. 2. Whole Hydroxylation Proteome Response upon MK-8617 Treatment

A. Overview of the workflow of the quantitative proteomic experiments. MCF10A cells were treated with MK-8617 (5 μM) upon indicated time point. Cell lysis were collected and subjected to TMT6-mass spectrometry analysis.

B. HIF1a level were measured using western blot upon MK-8617 (5 μM) treatment at indicated time points. GAPDH as the internal control.

(C-D). TMT results of HIF1a and BNIP3 in MCF10A cells upon MK-8617 (5 μM) treatment of the indicated time points.

E. Real-time RT-PCR analyses of HIF1a and BNIP3 in HEK293T and Hela cells upon MK-8617 (5 μM) treatment at indicated time point. Data are shown as mean ± SEM.

F. Hierarchical clustering of protein hydroxylation profiles of MCF10A cells upon MK-8617 (5 μM) treatment at the indicated time point. The whole hydroxylation proteome decreased upon MK-8617 treatment.

G. Motif analysis of hydroxylation peptide were analyzed using website tool: "https://meme-suite.org/meme/tools/meme". The hydroxylation peptides were identified using TMT6-MS.

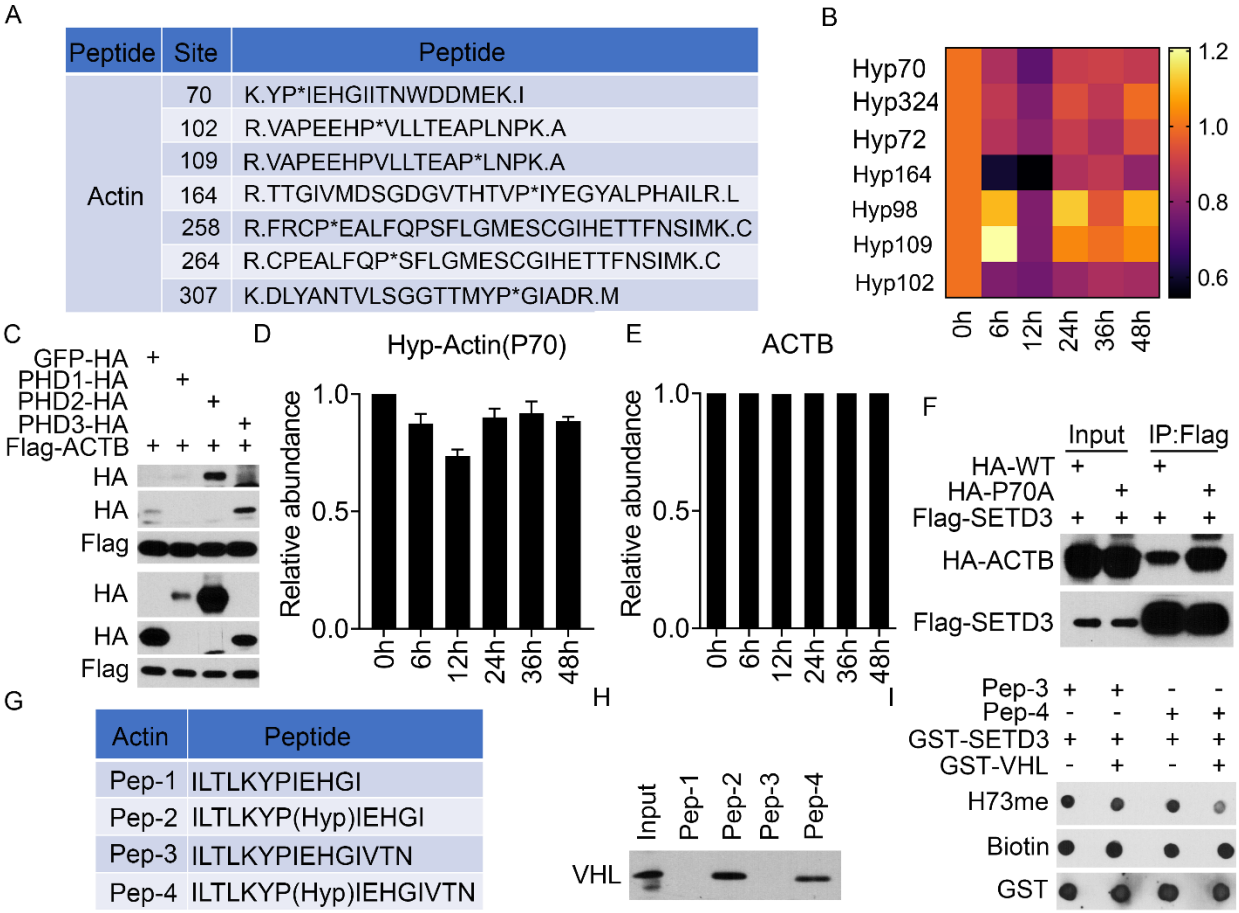

Fig. 3. VHL binds to Pro70-hydroxylated Actin and inhibit His73 Methylation

A. Actin hydroxylation proline site and peptide identified by TMT6-MS experiment.

B. The level of hydroxylated-proline site in actin identified by TMT6-MS experiment upon MK-8617 (5 μM) treatment as the indicated time point.

C. Actin interacts with PHD2 and PHD3. Flag-tagged actin was co-transfected with HA tagged GFP, PHD1, PHD2 and PHD3 into HEK293T cells. The lysates were subjected to immunoprecipitation using the anti-Flag beads. PHD1-3 were probed using an antibody against the HA-tag.

(D-E). TMT results of Hyp70-actin and actin in MCF10A cells upon MK-8617 (5 μM) treatment of the indicated time points.

F. Pro70 mutant of actin blocks the interaction of SETD3 and actin. HA-tagged actin (wild type and P70A mutant) was co-transfected with Flag-tagged SETD3 into HEK293T cells. The lysates were subjected to immunoprecipitation using the anti-Flag beads. HA-actin (WT and P70A mutant) were probed using an antibody against the HA-tag.

G. The peptides sequence synthesized, including non hydroxylated and hydroxylated (Hyp70) peptide.

H. VHL interacts with hydroxylated Pro70-actin peptide but not the non-hydroxylated peptide. The peptides were incubated with cell lysis from HEK293T cells, and were subjected to streptavidin beads.

I. VHL blocks H73 methylation in the hydroxylated (Pro70) peptide. In vitro methylation

assay with synthesized WT and Hydroxylated (Pro70) peptides.

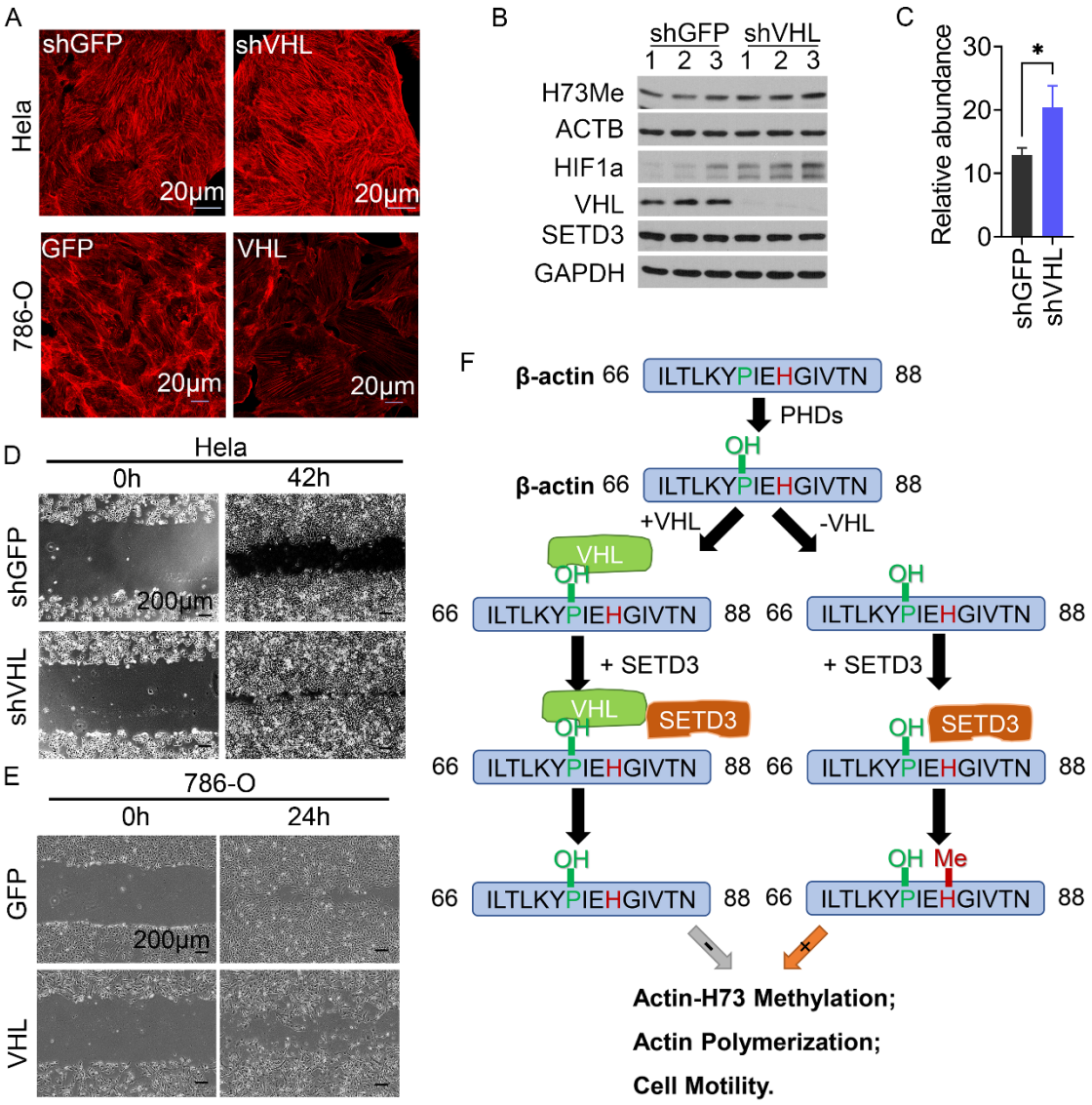

Fig. 4. VHL regulates cell motility through regulating H73Me

A. VHL regulate the level actin polymerization. VHL knockdown increases β-actin polymerization in Hela cells while VHL overexpress decrease β-actin polymerization in 786-O cells. Cells were fixed, permeabilized, stained with TRITC–conjugated phalloidin, and imaged by fluorescence microscopy. Scale bar, 20 μm.

(B-C). VHL knockdown increases H73Me and HIF1a level in Hela cells. Cell lysis were subjected to western blot (B) and H73Me level were quantified (C). GAPDH were used as the control. Data are shown as mean ± SEM, n=3 each group.

(D-E). VHL regulates cell motility. VHL knockdown increases cell motility in Hela cells while VHL overexpress decreases cell motility in 786-O cells. Representative images at indicated time points from two independent experiments. Scale bar, 200 μm.

F. The model of the mechanism about hydroxylation and VHL in regulating H73Me of actin, actin polymerization and cell motility.

Experimental procedures:

Chemicals and Antibodies

MK-8617 was purchased from Selleckchem (S8443), used at 5 μM final concentration; TRITC–conjugated phalloidin was purchased from (P1951), used at 1ug/ml, Isopropyl-β-D-thiogalactopyranoside (IPTG) (Dioxane-free) (Fisher Scientific, BP1755). β-Actin (13E5) Rabbit mAb (Cell Signaling, 4970s), Anti-H73Me antibody was provided by Dr. Or Gozani, Stanford University School of Medicine; Anti-GAPDH (Thermo Fisher Scientific, AM43000), HIF-1α Antibody (Cell Signaling, 3716s), VHL antibody (Cell Signaling, 68547s), SETD3 Antibody (Bethyl laboratories, A304-072A), PHD-2/Egln1 (D31E11) Rabbit mAb (Cell Signaling, 4835s), EGLN3/PHD3 Antibody (Novus Biologicals, NB100-139), Anti-CUL-2 Antibody (C-4) (Santa Cruz, sc-166506), Anti-Flag (Sigma, F7425), Anti-Flag (Sigma, F1804), Anti-HA (Cell Signaling Technology, 3724s), Donkey anti Rabbit IgG (GE healthcare, NA9340), Goat anti Mouse IgG (Millipore, AP181P), Monoclonal Anti-HA−Agarose (Sigma Aldrich, A-2095), ANTI-FLAG M2 Affinity Gel (Sigma Aldrich, A2220), GST (26H1) Mouse mAb (Cell Signaling, 2624s), HRP-Conjugated Streptavidin (Thermo Fisher, 21130).

Cell Culture

Hela (ATCC,), and HEK293T cells were cultured in Dulbecco’s modified Eagle’s medium (DMEM, sigma, D5796) supplemented with 10% fetal bovine serum (FBS, sigma, 12306C) and antibiotics (Gibco, 15240112) at 37 ℃ in a 5% CO2 incubator.

786-O, and RCCJF cells were cultured in RPMI-1640 medium (sigma, R8758) supplemented with 10% fetal bovine serum (FBS, sigma, 12306C) and antibiotics (Gibco, 15240112) at 37 ℃ in a 5% CO2 incubator.

HEK293T cells were cultured to 50–70% confluency in 10 cm dishes, and were then transfected using Lipofectamin-2000 (Sigma). The Plenti or pLKO.1 plasmid, VSVG, and delta8.9 were co-transfected at 8 μg, 6 μg, and 4 μg, respectively. The medium was changed 6 hours after the transfection. Viruses were collected twice at 24 h and 48 h after the transfection. Subsequently, 1 mL of virus was added to each well of Hela or 786-O cells in 6-well plates with Polybrene at a final concentration of 8 μg ml-1. After splitting the cells once, cells were infected with virus again using the same procedure. The medium was replaced after 48 h with a fresh growth medium containing 2 μg ml-1 blasticidin or puromycin.

Tandem Mass Tags (TMT) Mass Spectrometry

After the compound treatment, the cells were lysed using 1% SDS lysis buffer (1% SDS, 10 mM HEPES, pH 7.0, 2 mM MgCl2, 20 U ml-1 universal nuclease with added protease inhibitors and phosphatase inhibitors). Protein lysates were reduced by 2 mM dithiothreitol, and alkylated by adding iodoacetamide to a final concentration of 50 mM, followed by incubation in the dark for 20 min. The lysates were extracted by methanol-chloroform-precipitation and the proteins were solubilized in 8 M urea, then digested with Lys-C. The samples were then diluted to a final concentration of 2 M urea by the addition of 100 mM ammonium bicarbonate (pH 7.8). Proteins were digested overnight with sequencing-grade trypsin at a 1:100 (enzyme/substrate) ratio. Digestion was quenched by the addition of trifluoroacetic acid to a final concentration of 0.1%. For TMT MS samples, peptides were desalted using SepPak C18 columns (Waters) according to the manufacturer's instructions. Peptides were fractionated by using an off-line two-dimensional SCX-RP-HPLC (strong-cation-exchange reversed-phase HPLC) protocol. The sample were desalt using stage tips and subjected to MS analysis.

The MS samples were analyzed by LC-MS/MS experiments on an LTQ Velos Pro Orbitrap mass spectrometer (Thermo) using a top-20 CID (collision-induced dissociation) method. MS/MS spectra were searched against a composite database of the human protein database and its reversed complement using the Sequest algorithm. Search parameters allowed for a static

modification of 57.02146 Da for cysteine and a dynamic modification of oxidation (15.99491 Da) on methionine, respectively. Search results were filtered to include <1% matches to the reverse database by the linear discriminator function using parameters including Xcorr, dCN, missed cleavage, charge state (exclude 1C peptides), mass accuracy, peptide length and fraction of ions matched to MS/MS spectra. Peptide quantification was performed by using the Core Quant algorithm (20).

Immunoblot Analysis

For immunoblot analysis, the cells were lysed using 1% SDS lysis buffer (1% SDS, 10 mM HEPES, pH 7.0, 2 mM MgCl2, 20 U ml-1 universal nuclease with added protease inhibitors and phosphatase inhibitors). Protein concentrations were measured using the BCA assay (23227, Thermo Fisher). The lysates were mixed with the 4X reducing buffer (60 mM Tris-HCl, pH 6.8, 25% glycerol, 2% SDS, 14.4 mM 2-mercaptoethanol, 0.1% bromophenol blue). Samples were boiled for 10 min and the same amounts of proteins were subjected to electrophoresis using the standard SDS-PAGE method. Proteins were then transferred to a 0.22 μm nitrocellulose membrane (GE, 10600001), and were blocked with a TBST buffer (25 mM Tris-HCl, pH7.5, 150 mM NaCl, 0.05% Tween-20) containing 3% non-fat dried milk and incubated overnight with primary antibodies (1:1,000 dilution) at 4 °C and for 1h at room temperature with peroxidase-conjugated secondary antibodies (1:10000 dilution). Blots were developed using enhanced chemiluminescence and were exposed on autoradiograph films and were developed using standard methods.

The results were quantified using Image J and analyzed using Prism GraphPad Software.

In Vitro Methylation Assay

In vitro methyltransferase reactions were performed with 5 μg SETD3, 10 μg substrate peptide (hydroxylated or non-hydroxylated peptide), with/out VHL protein and 80 μM SAM (S-adenosylmethionine) in a buffer that contained 50 mM Tris pH 8.0, 20 mM KCl and 5 mM $MgCl_2$ and were incubated at 30 °C overnight. Reactions were resolved by dot blot analysis.

CO-Immunoprecipitation Assay

HEK293T cells were rinsed once with ice-cold PBS 24-36 hours after the transfection and lysed in the ice-cold BLB lysis buffer (10 mM KPO4, pH 7.6, 6 mM EDTA, pH 8.0, 10 mM MgCl2, 0.5 % NP-40, 0.1 % BriJ-35, 0.1 % DOC, adjust pH to 7.4) or IP buffer (0.5% NP-40, 150 mM NaCl, 50 mM Tris-HCl, pH 7.5) added with EDTA-free protease inhibitors (Roche). The soluble fractions from cell lysates were isolated by centrifugation at 13,000 rpm for 10 minutes. For immunoprecipitations, 20 μl of a 50% slurry of anti-FLAG (A2220, Sigma) or anti-HA beads (A2095, Sigma) were added to each lysate and incubated with rotation for overnight at 4°C. Immunoprecipitants were washed three times with BLB lysis buffer. Immunoprecipitated proteins were denatured by the addition of 100 μl of sample buffer and boiling for 10 minutes and subjected to immunoblot analysis.

For the peptide and VHL co-immunoprecipitation assay, peptide (hydroxylated or no-hydroxylated peptide) were incubated with streptavidin beads for 1 hour, then incubated with HEK293T cell lysis for 2 hours. After 3 times washing, the sample were subjected to western blot analysis.

Immunostaining Assay

Cells were plated on micro cover glasses (Electron Microscopy Sciences 72226-01). After confluence, cells were washed with PBS and fixed with 4% paraformaldehyde (PFA) in PBS for 10 min. The cells were permeabilized (0.2% Triton X-100, 10 min), blocked in 3% BSA (Sigma, A9418), then incubated with Phalloidin–Tetramethylrhodamine B isothiocyanate (P1951) for one hour at room temperature. After the incubation with primary antibodies, slides were washed for three times, then stained with DAPI (Sigma, D9542), and sealed with mounting medium (FluorSave reagent, Millipore, 345789). Photomicrographs were taken of representative 10×, 20× or 40× magnification fields using confocal microscope (Confocal Zeiss LSM880 Airyscan).

Cell Scratch Assay

Cells were seeded onto 6 well plate and cultured overnight to reach 50% confluence. The cell layer was scratched with a sterile 1-ml pipette tip, labeled, and photographed at the indicated time points with microscope.

qPCR analysis of target gene expression

Hela or HEK293T cells were lysed with TRIzol (Thermo Fisher Scientific) after MK-8617 treatment for indicated time point. Total RNA was extracted according to the manufacturer's instructions. The RNA was reverse transcribed with SuperScript™ III One-Step RT-PCR System (Thermo Fisher). Real-time RT-PCR experiments were performed using a Power SYBR™ Green PCR Master Mix (Thermo Fisher). The following primers were used for the qPCR reactions: Actin: F 5'-AAATCGTGCGTGACATTAAGGA-3' and R 5'-GCCATCTCTTGCTCGAAGTC-3'; HIF-1a: F 5'- TATGAGCCAGAAGAACTTTTAGGC-3' and R 5'- CACCTCTTTTGGCAAGCATCCTG-3'; BNIP3: F 5'-TCAGCATGAGGAACACGAGCGT-3' and R 5'- GAGGTTGTCAGACGCCTTCCAA-3'.

1. Zurlo, G., Guo, J., Takada, M., Wei, W., and Zhang, Q. (2016) New Insights into Protein Hydroxylation and Its Important Role in Human Diseases. *Biochim Biophys Acta* **1866**, 208-220
2. Semenza, G. L. (2001) HIF-1, O(2), and the 3 PHDs: how animal cells signal hypoxia to the nucleus. *Cell* **107**, 1-3
3. Gossage, L., Eisen, T., and Maher, E. R. (2015) VHL, the story of a tumour suppressor gene. *Nat Rev Cancer* **15**, 55-64
4. Lv, X., Li, J., Zhang, C., Hu, T., Li, S., He, S., Yan, H., Tan, Y., Lei, M., Wen, M., and Zuo, J. (2017) The role of hypoxia-inducible factors in tumor angiogenesis and cell metabolism. *Genes Dis* **4**, 19-24
5. Schofield, C. J., and Ratcliffe, P. J. (2004) Oxygen sensing by HIF hydroxylases. *Nat Rev Mol Cell Biol* **5**, 343-354
6. Debenham, J. S., Madsen-Duggan, C., Clements, M. J., Walsh, T. F., Kuethe, J. T., Reibarkh, M., Salowe, S. P., Sonatore, L. M., Hajdu, R., Milligan, J. A., Visco, D. M., Zhou, D., Lingham, R. B., Stickens, D., DeMartino, J. A., Tong, X., Wolff, M., Pang, J., Miller, R. R., Sherer, E. C., and Hale, J. J. (2016) Discovery of N-[Bis(4-methoxyphenyl)methyl]-4-hydroxy-2-(pyridazin-3-yl)pyrimidine-5-carboxami de (MK-8617), an Orally Active Pan-Inhibitor of Hypoxia-Inducible Factor Prolyl Hydroxylase 1-3 (HIF PHD1-3) for the Treatment of Anemia. *J Med Chem* **59**, 11039-11049
7. Maxwell, P. H., and Eckardt, K. U. (2016) HIF prolyl hydroxylase inhibitors for the treatment of renal anaemia and beyond. *Nat Rev Nephrol* **12**, 157-168
8. Chowdhury, R., Candela-Lena, J. I., Chan, M. C., Greenald, D. J., Yeoh, K. K., Tian, Y. M., McDonough, M. A., Tumber, A., Rose, N. R., Conejo-Garcia, A., Demetriades, M., Mathavan, S., Kawamura, A., Lee, M. K., van Eeden, F., Pugh, C. W., Ratcliffe, P. J., and Schofield, C. J. (2013) Selective small molecule probes for the hypoxia inducible factor (HIF) prolyl hydroxylases. *ACS Chem Biol* **8**, 1488-1496
9. Rabinowitz, M. H. (2013) Inhibition of hypoxia-inducible factor prolyl hydroxylase domain oxygen sensors: tricking the body into mounting orchestrated survival and repair responses. *J Med Chem* **56**, 9369-9402

10. Gupta, N., and Wish, J. B. (2017) Hypoxia-Inducible Factor Prolyl Hydroxylase Inhibitors: A Potential New Treatment for Anemia in Patients With CKD. *Am J Kidney Dis* **69**, 815-826
11. Pollard, T. D., and Cooper, J. A. (2009) Actin, a central player in cell shape and movement. *Science* **326**, 1208-1212
12. Dominguez, R., and Holmes, K. C. (2011) Actin structure and function. *Annu Rev Biophys* **40**, 169-186
13. Terman, J. R., and Kashina, A. (2013) Post-translational modification and regulation of actin. *Curr Opin Cell Biol* **25**, 30-38
14. Wilkinson, A. W., Diep, J., Dai, S., Liu, S., Ooi, Y. S., Song, D., Li, T. M., Horton, J. R., Zhang, X., Liu, C., Trivedi, D. V., Ruppel, K. M., Vilches-Moure, J. G., Casey, K. M., Mak, J., Cowan, T., Elias, J. E., Nagamine, C. M., Spudich, J. A., Cheng, X., Carette, J. E., and Gozani, O. (2019) SETD3 is an actin histidine methyltransferase that prevents primary dystocia. *Nature* **565**, 372-376
15. Guo, Q., Liao, S., Kwiatkowski, S., Tomaka, W., Yu, H., Wu, G., Tu, X., Min, J., Drozak, J., and Xu, C. (2019) Structural insights into SETD3-mediated histidine methylation on beta-actin. *Elife* **8**
16. Li, Z. L., Lv, L. L., Wang, B., Tang, T. T., Feng, Y., Cao, J. Y., Jiang, L. Q., Sun, Y. B., Liu, H., Zhang, X. L., Ma, K. L., Tang, R. N., and Liu, B. C. (2019) The profibrotic effects of MK-8617 on tubulointerstitial fibrosis mediated by the KLF5 regulating pathway. *FASEB J* **33**, 12630-12643
17. Luo, W., Lin, B., Wang, Y., Zhong, J., O'Meally, R., Cole, R. N., Pandey, A., Levchenko, A., and Semenza, G. L. (2014) PHD3-mediated prolyl hydroxylation of nonmuscle actin impairs polymerization and cell motility. *Mol Biol Cell* **25**, 2788-2796
18. Varland, S., Vandekerckhove, J., and Drazic, A. (2019) Actin Post-translational Modifications: The Cinderella of Cytoskeletal Control. *Trends Biochem Sci* **44**, 502-516
19. Venne, A. S., Kollipara, L., and Zahedi, R. P. (2014) The next level of complexity: crosstalk of posttranslational modifications. *Proteomics* **14**, 513-524
20. Zi, Z., Zhang, Y., Zhang, P., Ding, Q., Chu, M., Chen, Y., Minna, J. D., and Yu, Y. (2020) A Proteomic Connectivity Map for Characterizing the Tumor Adaptive Response to Small Molecule Chemical Perturbagens. *ACS Chem Biol* **15**, 140-150